PCCP

Accepted Manuscript

ROYAL SOCIETY OF CHEMISTRY

www.rsc.org/pccp

Cite this: DOI: 10.1039/c0xx00000x

www.rsc.org/xxxxxx

ARTICLE TYPE

A non-fullerene electron acceptor based on fluorene and diketopyrrolopyrrole building blocks for solution-processable organic solar cells with an impressive open-circuit voltage

Hemlata Patil,[a] Wang Xi Zu,[b] Akhil Gupta,*[ac] Vijila Chellappan[b], Ante Bilic,[d] Prashant Sonar,*[be] Anushri Rananaware,[a] Sidhanath V. Bhosale,[f] Sheshanath V. Bhosale*[a]

Received (in XXX, XXX) XthXXXXXXXXX 20XX, Accepted Xth XXXXXXXXX 20XX
DOI: 10.1039/b000000x

A novel solution-processable non-fullerene electron acceptor 6,6'-(5,5'-(9,9-dioctyl-9*H*-fluorene-2,7-diyl)bis(thiophene-5,2-diyl))bis(2,5-bis(2-ethylhexyl)-3-(thiophen-2-yl)pyrrolo[3,4-*c*]pyrrole-1,4(2*H*,5*H*)-dione) (DPP1) based on fluorene and diketopyrrolopyrrole conjugated moieties was designed, synthesized and fully characterized. DPP1 exhibited excellent solubility and high thermal stability which are essential for easy processing. Upon using DPP1 as an acceptor with the classical electron donor poly(3-hexylthiophene), solution processable bulk-heterojunction solar cells afforded 1.2% power conversion efficiency with a high open-circuit voltage (1.1 V). As per our knowledge, this value of open circuit voltage is one of the highest values reported so far for a bulk-heterojunction device using DPP1 as a non-fullerene acceptor.

In academic and industry sector, organic bulk-heterojunction (BHJ) solar cell research has gained momentum in view of their potential for the fabrication of low-cost, light weight and flexible photovoltaic devices.[1] Power conversion efficiencies (PCEs) over 9% for polymer- and small molecule-based BHJ devices have been achieved.[2] Donor functionalities such as conventional semiconducting polymers [poly(3-hexylthiophene) (P3HT)] and other donor-acceptor semiconducting polymers and small organic molecules have been examined in conjunction with soluble fullerene derivatives such as [6,6]-phenyl-C_{61}-butyric acid methyl ester ($PC_{61}BM$) as an electron acceptor material for achieving higher performance.[3] Much attention has been given to the design and development of donor materials whereas there is not much work that has been done so far on the electron accepting materials.[4] With regard to electron acceptor materials, fullerenes and their derivatives, such as $PC_{61}BM$ and $PC_{71}BM$, are the most common acceptors of choice mainly due to their superior electron affinity and good electron mobility.[5] However, fullerenes suffer from a number of disadvantages, such as high cost, weak absorption in the visible spectrum, restricted electronic tuning via synthesis and cumbersome purification. Also, a large electron affinity of fullerene derivatives can yield a low open-circuit voltage (V_{oc}) of the photovoltaic devices.[6] The above addressed issues with fullerenes provides a strong incentive to explore novel, easily processable and cheap non-fullerene electron acceptors. In order to design the new acceptor structures, we have to take an account of some of the important features such as strong and broad absorption, adequate solubility, high charge carrier mobility and appropriate energy levels.

Recently, non-fullerene electron acceptors have been developed [7] and PCEs exceeding 2% and 4% have been achieved using archetypal P3HT and non-P3HT donors, respectively.[8] Even though this progress is encouraging, considerable scope still exists to develop new non-fullerene acceptors which possess a strong optical absorption and good photochemical stability. Recently, the fluorene (FL) has been used as one of the promising building blocks for synthesizing potential electron-deficient non-fullerene electron acceptors.[8c] Amongst various electron deficient building blocks, a fused aromatic electron withdrawing diketopyrrolopyrrole (DPP) functionality has been proved to be one of the most promising moiety for synthesizing donor-acceptor based small molecular electron acceptors for BHJ devices.[7] It was envisaged that the combination of FL as donor and DPP unit as an acceptor could provide highly conjugated donor-acceptor chromophores with good planarity, high thermal stability, better electron affinity and enhanced solubility *via* attachment of preferred alkyl substituents. Our group has already developed promising *p*-type photoactive materials for solution-processable organic photovoltaic devices.[9]

Herein, we report the synthesis of a novel non-fullerene electron acceptor 6,6'-(5,5'-(9,9-dioctyl-9*H*-fluorene-2,7-diyl)bis(thiophene-5,2-diyl))bis(2,5-bis(2-ethylhexyl)-3-(thiophen-2-yl)pyrrolo[3,4-*c*]pyrrole-1,4(2*H*,5*H*)-dione) based on FL as a central core with DPP substituents (**DPP1**; as shown in Fig. 1) end capped at the both ends.

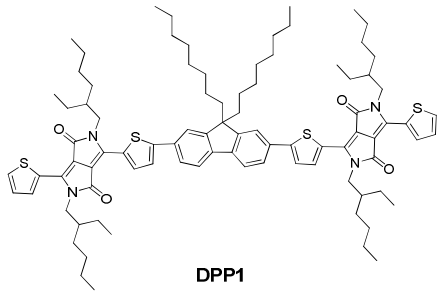

Fig. 1 Molecular structure of the investigated non-fullerene electron acceptor chromophore **DPP1**.

DPP1 has been used as an electron acceptor along with classical electron donor P3HT for solution-processable BHJ devices. Compound **DPP1** was synthesized in a straightforward manner with high yield *via* Suzuki coupling reaction between commercially available (9,9-dioctyl-9*H*-fluorene-2,7-diyl)diboronic acid (**1**) and 3-(5-bromothiophen-2-yl)-2,5-bis(2-ethylhexyl)-6-(thiophen-2-yl)pyrrolo[3,4-*c*]pyrrole-1,4(2*H*,5*H*)-dione (**2**). The reaction was conducted in dioxane:2M potassium carbonate (K_2CO_3) solvent mixture at 90 °C for 48 hours using tetrakis(triphenylphosphine)palladium(0) [$Pd(PPh_3)_4$] as a catalyst (Scheme 1). **DPP1** was worked up using conventional method and purified by simple column chromatography. The purity of the compound was confirmed by mass spectrometry (MS), ^1H and ^{13}C NMR spectroscopy techniques (for synthetic details, see ESI). **DPP1** was found to be highly soluble in a variety of organic solvents such as chloroform, dichlorobenzene and toluene (for instance, 30 mg/mL in *o*-dichlorobenzene). High solubility is absolutely required for the fabrication of solution-processable roll to roll BHJ devices and **DPP1** fulfils this criterion.

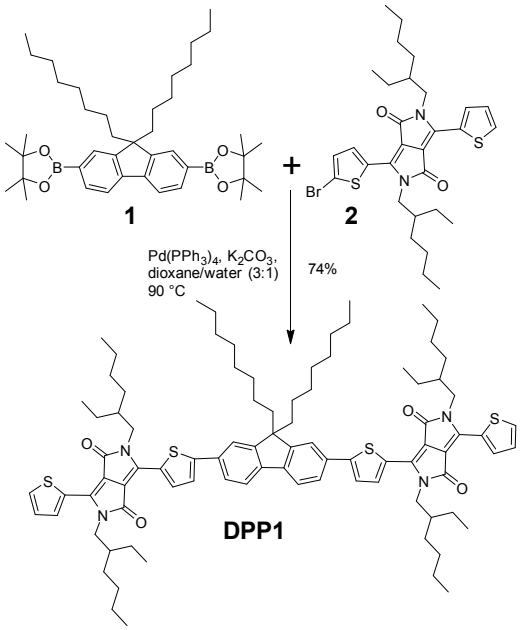

Scheme 1 Reaction strategy for the synthesis of **DPP1**

The normalized optical absorption spectra of **DPP1** in chloroform solution (8.7×10^{-7} M) and as a thin solid film are shown in Fig. 2. In solution, **DPP1** exhibits strong absorption with a maximum extinction coefficient of 13.4×10^4 M^{-1} cm^{-1} at 599 nm. As a thin film, **DPP1** shows a broad absorption peak throughout the visible region (400–700 nm) which is red-shifted by around 20 nm compared to its solution spectrum. Such a red shift is attributed with the solid state ordering of the molecule. The optical band gap was calculated from the tangent of the edge of longest wavelength (absorption cut-off) in thin solid film. This value was found to be 1.80 eV. We also measured the optical data for the P3HT:**DPP1** blend (in a ratio of 1:1 w/w and spin coated on a glass) as a thin film at room temperature and post-annealed at 150 °C (see Fig. 2).Thin films of blends of P3HT and **DPP1** show quenching of the photoluminescence (see Fig. S1 in ESI).

Theoretical density functional theory (DFT) calculations using the Gaussian 09 suite of programs[10] and B3LYP/6-311+G(d,p)//B3LYP/6-31G(d) level of theory indicated that orbital densities are evenly distributed over the whole molecular backbone of **DPP1** (see Fig. S2 in ESI). This finding is in consistent with the earlier reported best performing non-fullerene acceptor where FL moiety was also used as one of the building block.[8c]

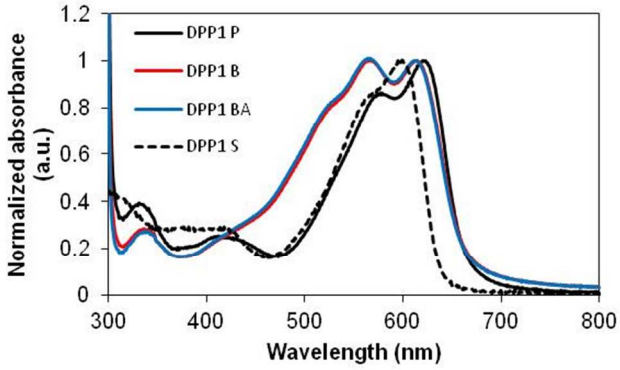

Fig. 2 UV-vis absorption spectra of pristine film (**DPP1 P**; solid black curve), in chloroform solution (**DPP1 S**; dotted black curve), 1: 1 P3HT: **DPP1** blend film (**DPP1 B**; red curve)and post-annealed (150 °C for 5 min) blend film (**DPP1 BA**; blue curve).

The highest occupied molecular orbital (HOMO) energy of **DPP1** was measured using photo electron spectroscopy in air (PESA) technique using the spin coated thin film of **DPP1** (Fig. S3 in ESI). The lowest unoccupied molecular orbital (LUMO) energy was calculated by taking the difference between optical bandgap and the HOMO value. The measured HOMO and LUMO energies were found to be -5.30 eV and -3.50 eV respectively. The difference between the LUMO of **DPP1** (-3.50 eV) and the HOMO of P3HT (-4.70 eV from PESA) is as large as 1.20 eV (theoretical open circuit voltage V_{oc}), which is promising for achieving a high V_{oc} in solar cells (Fig. 3 for energy level diagram).

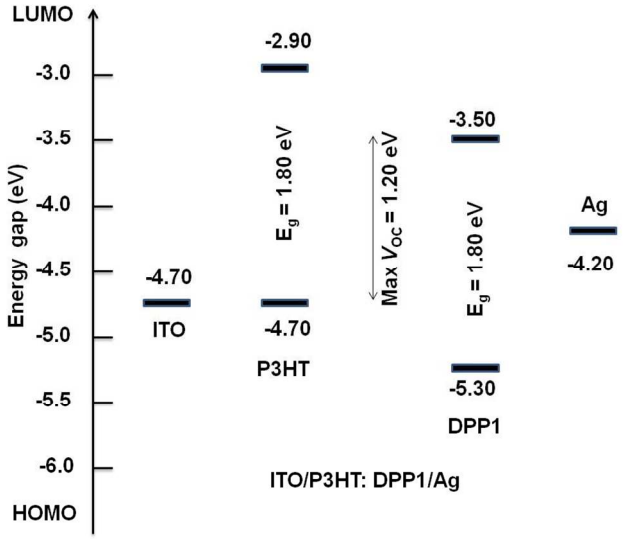

Fig. 3 Energy level diagram showing alignments of different components of BHJ device architecture

It was further realized that despite the presence of interesting and

lucrative optoelectronic properties, organic semiconducting materials must possess thermal stability so that they can endure rigid device fabricating conditions, such as device annealing at a higher temperature. In-line with this requirement, we conducted themrogravimetric analysis (TGA) analysis. TGA analysis established that **DPP1** exhibits excellent thermal stability and is stable up to 350 °C (Fig. S4 in ESI), a finding that supports high temperature annealing of P3HT: **DPP1** devices. In addition to TGA, we also conducted differential scanning calorimetry (DSC) analysis of **DPP1** to examine thermal transitions. DSC thermogram of **DPP1** indicates melting transition at around 259 °C (Fig. S5 in ESI). Initially, the newly synthesized **DPP1** was used as a non-fullerene acceptor (n-type) with classical donor polymer P3HT (p-type) for solution-processed BHJ OPV devices to test its performance. BHJ architectures typically deliver higher power conversion efficiencies (PCEs) by maximising the surface area of the interface between the p- and n-type materials in the active layer. The BHJ device structure used in this study was ITO/PEDOT:PSS (35 nm)/active layer/Ca (15 nm)/Ag (100 nm) where the active layer was a solution-processed blend of P3HT and **DPP1**. An initial screen of the efficacy of the target compound, **DPP1**, as a non-fullerene acceptor exhibits promising performance. The *J-V* characteristics are shown in Fig. 4 and the device performance is summarized in Table 1. Table 1 summarizes the photovoltaic cell parameters [short circuit voltage (V_{oc}), current density (J_{sc}), fill factor (FF), and PCE] for P3HT: **DPP1** blends.

Table 1 Photovoltaic properties of small area single cell modules based on blend layers of P3HT:**DPP1** with different processing conditions.

Sample (spin rate)	PCE (%)	V_{oc} (V)	J_{sc}(mA/cm^2)	FF (%)
3000 rpm	0.32	0.53	1.85	32
3000 rpm 150 °C 5mins [a]	0.09	0.22	1.52	28
2000 rpm	0.81	1.03	2.04	39
2000 rpm 150 °C 5mins[a]	1.20	1.10	2.42	45

[a] active layer annealing before depositing cathode.

Thermal annealing of devices at 150 °C showed an improvement in PCEs of about 50% when compared with as-casted devices. Overall, BHJ devices show significantly improved performance; V_{oc}, J_{sc}, FF and PCE reached 1.10 V, 2.42 mA/cm^2, 0.45 and 1.20%, respectively, when annealed at 150 °C for 2000 rpm spin coated blend film. These BHJ devices yielded very high V_{oc} as we expected, and it is notable that the V_{oc} of 1.1 V is among the highest values reported so far for a single BHJ device,[8,11] and can be attributed to a very large energy-gap (1.20 eV) between the LUMO of **DPP1** and the HOMO of P3HT. The thickness of active layer affects the J_{sc}, FF and V_{oc}. The FF and V_{oc} decrease rapidly when we increased the thickness of active layer by increasing concentration of donor-acceptor blend and decreasing a spin speed. This is due to the deposition of a very thick layer that can hamper the charge carrier mobility and the charge collection at the respective electrodes can slower down. In addition, the film morphology and uniformity of the film was not good enough to fabricate OPV device using lower spin speed. Lower spin speeds can generate thicker films and such kind of morphology is not favourable for higher performance. After optimizing device fabrication at 2000 rpm, 3000 rpm and 4000 rpm spin speeds; we got the best devices for blend films spun at 2000 rpm and 3000 rpm.

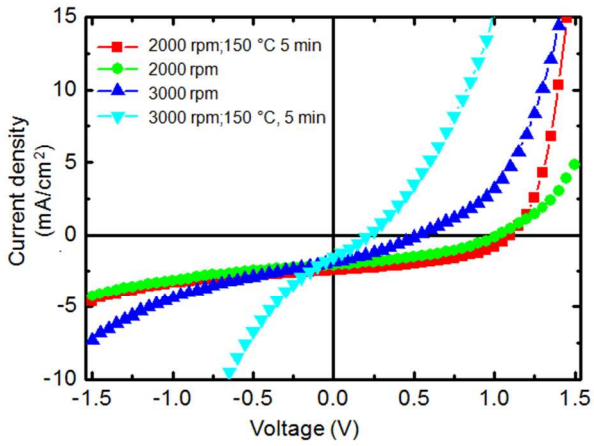

Fig. 4 Current-voltage (*J-V*) curves for devices based on **DPP1** in blends with P3HT (1:1 wt.) under simulated sunlight (AM 1.5, 1000 W/m^2). Device Structure is: ITO/PEDOT:PSS (35 nm)/active layer/Ca (15 nm)/Ag (100 nm).

Incident photon-to-current-conversion efficiency (IPCE) spectra of the devices (see Fig. 5) are consistent with the P3HT: **DPP1** blend film absorption and show broad IPCE from 300 to 700 nm with an IPCE maximum of ~17% at 580 and 620 nm. The lower J_{sc} of P3HT:**DPP1** blend system is also attributed with an overlay of **DPP1** and P3HT spectra. Higher J_{sc} is desirable if there is offset in absorption for p- and n-type materials. We believe that with other low band gap conjugated donor materials over a broad range of wavelengths, the higher PCE can be achieved.

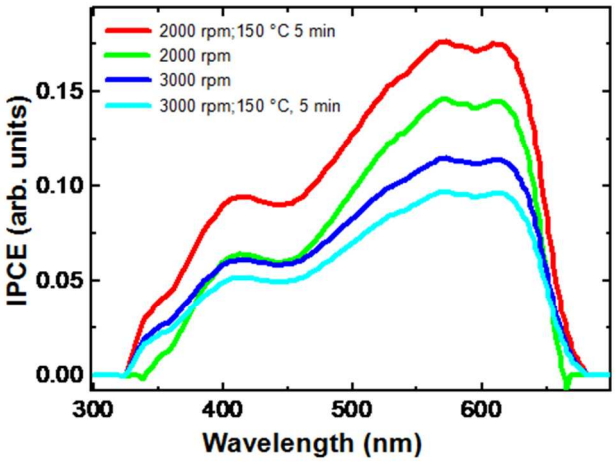

Fig. 5 IPCE spectra measured for P3HT:**DPP1** based OPV devices at various processing conditions.

We also investigated the surface microstructure of P3HT:**DPP1** blend thin film using atomic force microscopy (AFM) in its tapping mode (see Fig. 6).This study indicated the presence of

microcrystalline domains in the blend after annealing at 150 °C for 5 min. The crystalline grains grew larger at 150 °C and appeared clearly in AFM image. This ordering is affiliated with the self-organization of P3HT polymeric chains which is beneficial for effective charge transport. The root mean square (RMS) roughness values were measured and were found to be 8.2 nm and 2.1 nm, respectively, before and after annealing the blend film.

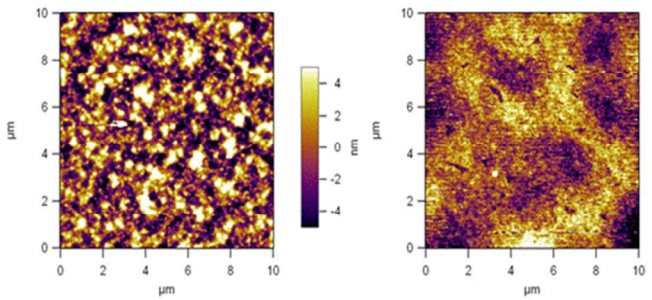

Fig. 6 AFM images for a thin film of P3HT:**DPP1** blend (left) and as-casted **DPP1** (right) annealed at 150 °C for 5 min (1: 1 blend in 1 mL *o*-DCB, 2000 rpm/s for 1 min).

For annealed film, the active layer becomes smoother which is primarily due to the removal of solvent and rearrangement of film during annealing process. These changes in morphology due to annealing of blend film reflect the improved device performance. Additionally, the tuning of morphological pattern at 150 °C is also consistent with the glass transition temperature of P3HT which is around 140 °C.[12] In an attempt to measure the charge carrier mobility of **DPP1**, a thin film of pristine **DPP1** was spin coated on self-assembled monolayer (SAM) treated Si/SiO_2 substrates and the mobility was measured using top contact bottom gate transistor geometry (see experimental for details in the ESI). No electron mobility was observed for the pristine **DPP1**, however, the hole mobility was measured to be 10^{-4} cm^2/Vs (see the transfer and output characteristics of OFETs in Fig. S6 in the ESI). The lack of electron mobility in pristine film might be related with the higher LUMO value of **DPP1** with respect to vacuum, electron traps at the dielectric-**DPP1** interface and lower electron affinity. We also probed the electron mobility of **DPP1** by time of flight photoconductivity (TOF-PC) method. The electron mobility was directly obtained from the integrated measurement on a simple diode structure of ITO/**DPP1** (400nm)/Al. The film was excited using a pulsed laser of wavelength 620 nm (pulse width <5 ns, 1Hz repetition rate). A negative voltage bias was applied across the device in order to measure the electron mobility. The TOF transients due to electrons are measured using an oscilloscope by varying the bias voltage. The detail of the TOF experimental set-up was elaborated elsewhere. [13, 14] The TOF measurements were carried out using integrated mode as the film thickness used in this measurement was 400 nm. The variation of total charge accumulated at the collecting electrode with respect to time is measured in integrated TOF-PC method. The time taken to collect the maximum charge (t_m) is estimated from the transient and the charge mobility (μ) was measured using the relation of $\mu = d^2/t_m V$, where d is the film thickness and V is the applied voltage. The advantage of TOF-PC method is that the charge mobility is independent of contacts and it allows the measurement of charge mobility in dispersive samples as well as in thin film samples. The details of integrated TOF-PC technique is elaborated in earlier work .[15] The TOF-PC transients measured are shown in the inset of Fig 7. The t_m was obtained from the transients and the calculated electron mobility for different electric field is shown in Fig. 7. The obtained electron mobility is in the range of 8 x 10^{-6} cm^2/Vs at an applied electric field of 1MV/cm.

Although the material reported in this study achieved very high V_{oc} with promising power conversion efficiency in OPV devices, the discovery of such materials exhibiting promising optoelectronic properties opens up the way to develop such motifs (based on the central FL functionality) and paves the way for such materials to be used for other organic electronic applications such as organic light-emitting diodes and organic field-effective transistors

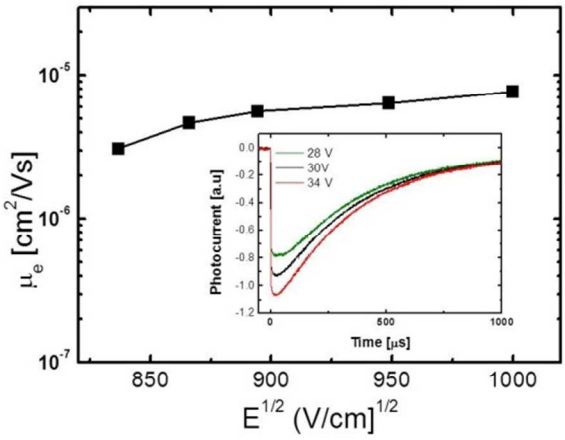

Fig. 7 Variation of electron mobility with applied electric field; Inset: current integrated TOF-PC transients for electrons measured for different applied voltages.

Conclusions

In summary, we have designed, synthesized and successfully developed a novel non-fullerene electron acceptor 6,6'-(5,5'-(9,9-dioctyl-9*H*-fluorene-2,7-diyl)bis(thiophene-5,2-diyl))bis(2,5-bis(2-ethylhexyl)-3-(thiophen-2-yl)pyrrolo[3,4-*c*]pyrrole 1,4(2*H*,5*H*)-dione) (**DPP1**) with fluorene (FL) as a central core and diketopyrrolopyrrole (DPP) units as the terminal substituents. **DPP1** was synthesized in one-pot via Suzuki coupling, has excellent solubility and thermal stability, strong and broad absorption and matching energy levels with P3HT. The BHJ devices based on a P3HT: **DPP1** blend (1:1) after annealing at 150 °C for 5 min yielded a notable PCE of 1.20 % and a very high V_{oc} of 1.10 V. The electron mobility of DPP1 was also measured 8 x 10^{-6} cm^2/Vs using time of flight photoconductivity (TOF-PC) method. Our results strongly support the excellent prospects of simple non-fullerene electron acceptors such as **DPP1**, and their future derived analogues, for applications in solution-processable OPV devices.

Acknowledgements

Sh. V. B. acknowledges financial support from the Australian Research Council under a Future Fellowship Scheme (FT110100152) and the School of Applied Sciences (RMIT University) for the facilities. The CSIRO Material Science and Engineering (CMSE) is acknowledged for providing support through a visiting fellow position (A.G.). A.B. thanks CSIRO for support through the Julius Career Award. The use of the NCI National Facility supercomputers at the ANU is gratefully acknowledged. W.X and P. S. thanks to the Institute of Materials Research and Engineering (IMRE), the Agency for Science, Technology and Research (A*STAR), and the "Printable high performance semiconducting materials for OPVs and OTFTs" for financial support.

Notes and references

[a]*School of Applied Sciences, RMIT University, GPO Box 2476V, Melbourne Victoria3001 Australia; Tel: +61 3 99252680; E-mail: sheshanath.bhosale@rmit.edu.au*

[b]*Institute of Materials Research and Engineering (IMRE), 3, Research Link, Singapore 117602*

[c] *Medicinal Chemistry, Monash Institute of Pharmaceutical Sciences, Monash University, Parkville Victoria 3052 Australia; Tel: +61 3 9903 9599; E-mail: akhil.gupta@monash.edu*

[d] *CSIRO Computational Informatics, Private Bag 33, Clayton South Victoria 3169 Australia.*

[e] *Current Address: School of Chemistry, Physics and Mechanical Engineering, Queensland University of Technology (QUT), GPO Box 2434, Brisbane , QLD 4001, Australia; E-mail: sonar.prashant@qut.edu.au*

[f] *Polymers and Functional Material Division, CSIR-Indian Institute of Chemical Technology, Hyderabad 50060, AP, India*

† Electronic Supplementary Information (ESI) available: [Synthetic details, experimental procedures, DFT calculations, PESA diagram, TGA and DSC curves]. See DOI: 10.1039/b000000x/

1 (*a*) S. Günes, H. Neugebauer and N. S. Sariciftci, *Chem. Rev.*, 2007, **107**, 1324; (*b*) B. C. Thompson and J. M. J. Frechet, *Angew. Chem. Int. Ed.*, 2008, **47**, 58.

2 (a) Z. He, C. Zhong, S. Su , M. Xu , H. Wu, Y. Cao, *Nat. Photon*. 2012, **6**, 593; (b) J. Zhou, Y. Zuo, X. Wan, G. Long, Q. Zhang, W. Ni, Y. Liu, Z. Li, G. He, C. Li, B. Kan, M. Li, Y. Chen, *J. Am. Chem. Soc*. 2013, **135**, 8484; (c) V. Gupta, A. K. K. Kyaw, D. H. Wang, S. Chand, G. C. Bazan and A. J. Heeger, *Sci. Rep.*, 2013, **3**, 1965.

3 (*a*) Y. Lin, Y. Li and X. Zhan, *Chem. Soc. Rev.*, 2012, **41**, 4245; (b) Y. Li, *Acc. Chem. Res*., 2012, **45**, 723; (c) J. Roncali, *Acc. Chem. Res.*, 2009, 42, 1719.

4 (a) P. -L. T. Boudreault, A. Najari, M. Leclerc, *Chem. Mater*. 2011, **23,** 456; (b) A. Gupta, S. E. Watkins, A.D. Scully, Th. B. Singh, G. J. Wilson, L. J. Rozanski, R. A. Evans, *Synth. Met*., 2011, **161**, 856; (c) C. J. Brabec, S. Gowrisanker, J. J. M. Halls, D. Laird, S. Jia, S. P. Williams, *Adv. Mater.*, 2010, **22**, 3839; (d) B. Walker, C. Kim, T.-Q. Nguyen, *Chem. Mater.,* 2011, 23, 470; (e) Y. Li, Q. Guo, Z. Li, J. Pei, W. Tian, *Energy Environ. Sci.,* 2010, **3** , 1427; (f) A. Mishra, P. Bäuerle, *Angew. Chem. Int. Ed*., 2012, **51**, 2020.

5 (a) F. G. Brunetti, X. Gong, M. Tong, A. J. Heeger, F. Wudl, *Angew. Chem. Int. Ed.*, 2010, **49**, 532; (b) F.G. Brunetti, R. Kumar, F. Wudl, *J. Mater. Chem.,* 2010, **20**, 2934.

6 R. Y. C. Shin, P. Sonar, P. S. Siew, Z. K. Chen, A. Sellinger, *J. Org. Chem.,* 2009, **74**, 3293.

7 (a) J. E. Anthony, *Chem. Mater.,* 2011, **23**, 583; (b) P. Sonar, J. P. Fong Lim, K. L. Chan, *Energy Environ. Sci.*, 2011, **4**, 1558; (c) P. Sonar, G. M. Ng, T. T. Lin, A. Dodabalapur, Z. K. Chen, *J. Mater. Chem.,* 2010, **20** 3626; (d) Y. Li, P. Sonar, L. Murphy, W. Hong, *Energy Environ. Sci.,* 2013, **6**, 1684; (e) C. B. Nielsen, M. Turbiez, I. McCulloch, *Adv. Mater.,* 2013, **25** 1859; (f) J. D. Yuen, F. Wudl, *Energy Environ. Sci*. 2013, **6**, 392; (g) B. P. Karsten, J. C. Bijleveld and R. A. J. Janssen, *Macromol. Rapid Commun*., 2010, **31**, 1554.; (h) Y. Lin, X. Zhan, *Mater. Horiz*. 2014, 10.1039/C4MH00042K; (i) Y. Lin, Y. Li and X. Zhan*, Adv. Energy Mater*., 2013, **3**, 724; (j) Y. Lin, P. Cheng, Y. Li and X. Zhan, *Chem. Commun*., 2012, **48**, 4773; (k) A. F. Eftaiha, J. P. Sun, I. G. Hill and G. C. Welch, *J. Mat. Chem. A,* 2014, **2**, 1201; (k) Y. Lin, Y. Wang, J. Wang, J. Hou, Y. Li, D. Zhu, X. Zhan, *Adv. Mater.*, 2014, DOI: 10.1002/adma.201400525; (l) Y. Lin, J. Wang, S. Dai, Y. Li, D. Zhu, X. Zhan, *Adv. Energy Mater*., 2014, DOI: 10.1002/aenm.201400420.

8 (a) J. T. Bloking, X. Han, A. T. Higgs, J. P. Kastrop, L. Pandey, J. E. Norton, C. Risko, C. E. Chen, J. -L. Brédas, M. D. McGehee, A. Sellinger, *Chem. Mater*. 2011, **23**, 5484; (b) Y. Lin,Y. Li, X. Zhan, *Adv. Energy Mater.* 2013, **3** 724; (c) K. N. Winzenberg, P. Kemppinen, F. H. Scholes, G. E. Collis, Y. Shu, Th. B. Singh, A. Bilic, C. M. Forsyth, S. E. Watkins, *Chem.Comm.,* 2013, **49** 6307; (d) C. H. Woo, T. W. Holcombe, D. A. Unruh, A. Sellinger, J. M. J.Fréchet, *Chem. Mater.,* 2010, **22**,1673; (e) Y. Zhou, L. Ding, K. Shi, Y.-Z. Dai, N. Ai, J. Wang, J. Pei, *Adv. Mater.,* 2012, **24,** 957; (f) T. Zhou, T. Jia, B. Kang, F. Li, M. Fahlman, Y. Wang, *Adv. Energy Mater*., 2011, **1**, 431; (g) X. Zhang, Z. Lu, L. Ye, C. Zhan, J. Hou, S. Zhang, B. Jiang, Y. Zhao, J. Huang, S. Zhang, Y. Liu, Q. Shi, Y. Liu and J. Yao, *Adv. Mater.*, 2013, **25**, 5791.

9 (a) A. Gupta, A. Ali, A. Bilic, M. Gao, K. Hegedus, B. Singh, S.E. Watkins, G. J. Wilson,U. Bach, R. A. Evans, *Chem. Comm*., 2012, **48**, 1889; (b) A. Gupta, V. Armel, W. Xiang, G. Fanchini, S. E. Watkins, D. R. MacFarlane, U. Bach, R. A. Evans, *Tetrahedron,* 2013, **69**, 3584; (c) R. J. Kumar, Q. I. Churches, J. Subbiah, A. Gupta, A. Ali, R. A. Evans, A. B. Holmes, *Chem. Comm.,* 2013, **49**, 6552; (d) A. Gupta, A. Ali, Th. B. Singh, A. Bilic, U. Bach, R. A. Evans, *Tetrahedron,* 2012, **68**, 9440.

10 M. J. Frisch et al., Gaussian 09 revision D.01, Gaussian Inc. Wallingford CT (2013).

11 Y. Lin, P. Cheng, Y. Li, X. Zhan, *Chem Comm*., 2012, **48**, 4773.

12 G. Li, V. Shrotriya, J. Huang, Y. Yao, T. Moriarty, K. Emery, Y. Yang, *Nat. Mater.*, 2005, **4**, 864.

13 M. J. Tan, W. P. Goh, L. Jun, G. Pundir, C. Vijila, C. Z. Kuan, *ACS Appl. Mater. Interface*., 2010, **2**, 1414.

14 C.Vijila, N. G. Meng , C. Z. Kuan, Z. Furong, C. S. Jin, *J. Polym. Sci. B Polym. Phys.*, 2008, **46**, 1159.

15 A. J. Campbell, D. D. C. Bradley, H. Antoniadis, *Appl. Phys. Lett.*, 2001,**79**, 2133.